



## Effect of fines on deformation and matric suction response of unbound granular base materials

Ovidiu Craciun

*Department of Civil Engineering – University of New South Wales at Australian Defence Force Academy, Canberra, ACT, Australia*

Sik-Cheung Robert Lo

*Department of Civil Engineering –University of New South Wales at Australian Defence Force Academy, Canberra, ACT, Australia*

### ABSTRACT

The influence of fines content on the behaviour of an unbound granular base (UGB) material has been studied experimentally by cyclic triaxial testing with up to  $2.8 \times 10^4$  load cycles per test. The framework of unsaturated soil mechanics with matric suction measurement was adopted in this study. The effect of dry density coupled with degree of saturation can be captured by matric suction. The evolution of resilient modulus, matric suction, axial and volumetric strain were studied. This approach implies the possible use of non-standard materials for pavement design with significant cost and environmental benefits.

### RÉSUMÉ

L'influence des amendes de contenu sur le comportement d'un non relié granulaire base (UGB) le matériel a été étudiée expérimentalement par des essais triaxiaux cycliques avec un maximum de  $2.8 \times 10^4$  cycles de charge par test. Le cadre de mécanique des sols non saturés avec du la suction matricielle mesure a été adoptée dans cette étude. L'effet de densité sèche de pair avec le degré de saturation peuvent être captés par des suction matricielle. Les évolutions des modules élastiques, suction matricielle, axial et volumétrique souche ont été étudiés. Cette approche implique l'utilisation éventuelle de non-matériaux standards pour la conception des chaussées avec des coûts et des avantages pour l'environnement.

### 1 INTRODUCTION

A layer of unbound granular base (UGB) material is often incorporated in a pavement system in order to provide load spreading ability and resistance to rutting. The former is related to material's stiffness, while the latter is characterised by the evolution of permanent deformation with load cycles.

A UGB material consists of well-graded sandy gravel with a small amount of fines (material passing 75  $\mu\text{m}$  sieve). This material is compacted generally close to the maximum dry density as measured in a standard Proctor test.

Traditional empirical design of road pavements is based on the use of high quality granular base materials with tightly specified limits for fines content. However, there are circumstances when UGB materials include a higher fines content than that required by normal specifications.

Published work focused on the effect of fines on UGB materials behaviour appears to be limited, and the findings are not necessarily consistent as discussed below.

In a study conducted by Hicks (1956) based on North Carolina road authority data base, it was emphasised that fines facilitate the "binding" of aggregate particles and therefore UGB materials should contain at least 5% fines. Hicks and Monismith (1971) however, suggested that the influence of fines on resilient modulus was dependent on material type. However, multi-stage testing in the form of applying multiple deviator stress levels to the same specimen was used. Therefore, the effect of deviatoric loading history (due to multi-stage testing) was not

considered. Thompson and Smith (1990) proposed to the Illinois road authority a drastic reduction of allowable fines contents from  $(12 \pm 4) \%$  to  $(2 \pm 2) \%$ . This was based mainly on the permanent deformation accumulation at 5000 load repetitions and that the resilient moduli measured in cyclic triaxial testing did not provide a clear distinction between materials. Note that resilient moduli were measured in multi-stage testing (different deviator stress levels) after the 1<sup>st</sup> 5000 cycles. Haynes and Yoder (1963) studied the behaviour of gravel aggregates with different percentages of fines (6.2 %, 9.1 % and 11.5 %) by cyclic triaxial testing. Their work showed that the least favourable behaviour (in terms of resilient modulus and permanent deformation) occurred at a fines content of 9.1 %. Their work also showed that the accumulation of permanent deformation after 1000 load cycles, increased rapidly as the degree of saturation exceeded 85 %, irrespective of fines content. However, their studies suggested that resilient moduli measured after 1000 load cycles manifested a linear decrease with degree of saturation in the range of 70 % to 98 %. Ashtiani et al. (2007) observed that for an UGB material wet of optimum moisture content, the stiffness anisotropy dramatically decreased with increased fines content.

An important consideration is that maximum dry density is dependent on fines content. However, the fines content that provides the highest maximum dry density does not coincide with that of highest strength as reported in (Yoder and Woods 1946, Kalcheff 1974,). It is worth mentioning that the former was based on penetration resistance (measured in a way similar to a CBR test) while the latter was measured in monotonic triaxial tests. There are also

concerns presented in the literature that higher fines content may lead to increased sensitivity to moisture content (Fwa 1987, Thom and Brown 1988, Thompson and Smith 1990, Chen et al. 2006).

It is evident that existing publications do not give a simple picture of the influence of fines. It is noted that the number of load cycles used per test were relatively low, and that different studies used different bases of comparison.

The objective of this paper is to study systematically the influence of fines on UGB behaviour by taking into account the following issues:

- Both resilient modulus and permanent deformations are measured in the same test, and that the significantly higher number of load cycles were applied in each test.
- Multi-stage test was not used to eliminate the possible effect of stress history
- The test results were analysed using an unsaturated soil mechanics framework. This necessitates matric suction measurement.

The use of matric suction measurement in cyclic triaxial testing has rarely been reported in literature. The matric suction of a specimen can also capture the coupled effect of dry density and degree of saturation.

## 2 MATERIAL TESTED

A well-graded high quality crushed rock was used for this study. The largest particle size was 19 mm and the fines content was 10 %. The specimens were formed at 100 % maximum dry density, and the resultant material is denoted as **UGB-0**. A synthetic material with additional fines was created by introducing an extra 10 % fines to the original one. These additional fines were extracted from tested specimens of the original material. The synthetic material with additional fines is denoted **UGB-a** when compacted to the maximum dry density of the material with additional fines, and **UGB-b** when compacted to a density equal to that of the original one (i.e. **UGB-0**). The index properties of these materials are presented in Table 1.

Table 1. Index properties

Material	Fines(%)	OMC(%)	MDD	Gs
UGB-0	10	5.1	2.313	2.96
UGB-a,b	20	6.4	2.51	2.97

Notes:

Fines Properties (%): Liquid Limit, (LL) = 28; Plastic Limit, (PI) = 26; Plasticity Index, (PI) = 2.

OMC = Optimum Moisture Content

MDD = Maximum Dry Density

Gs = Specific Gravity

## 3 UNSATURATED TESTING METHODOLOGY

A state-of-the-art cyclic triaxial station has been used for this study. The special features of this testing system are discussed below.

### 3.1 Measurement system

The axial load was measured by an internal load cell placed inside the triaxial chamber in order to eliminate ram friction error, which is more pronounced in cyclic loading tests (Chen 1997, Lo 1999, Wardani 1999). "On sample" transducers were adopted for strain measurements. Two diametrically opposed miniature Linear Variable Differential Transducers (LVDT-s) were used for axial displacement measurement. A Hall Effect radial caliper mounted at the mid-height of the specimen was used for measurement of radial displacement.

Negative pore water pressure was measured utilising a ceramic disk with high air entry (HAE) value (at the bottom platen) and a low compliance pressure transducers in line. The applicability of ceramic disks as a direct measurement of pore water pressure in an air-water mixture was discussed in Fredlund and Rahardjo (1993). The pore air pressure was measured via a porous disk at the top platen. The matric suction,  $u_a - u_w$  (i.e. defined by the difference between the pore air pressure,  $u_a$  and the pore water pressure,  $u_w$ ) can then be monitored at all stages. As matric suction was expected to be low, ceramic disk with a 100 kPa Air Entry Value was used and the axis translation technique (Hilf 1965) was not necessary. The air line connected at the top platen was open to the atmosphere at all times via a "U" trap to verify that no water movement occurred via the top drainage line.

### 3.2 Bottom Platen Design

The bottom platen was designed to enable the measurement and monitoring of matric suction evolution during cyclic loading. In particular, it ensured proper saturation (at all stages during specimen preparation) and regular maintenance of the ceramic disk. Details of the special platen, fitted with a ceramic disk are given in Craciun et al. (2007).

### 3.3 Specimen Compaction and Preparation

A specimen of 100 mm diameter by 200 mm height was compacted in a three-piece split compaction mould that incorporated the bottom platen (Chen, 1997). The ceramic disk and drainage lines of the bottom platen were saturated by immersing in de-aired water under 70-90 kPa vacuum for at least 24 hours before placement into the compaction mould. Saturation was maintained during compaction as the connection screw of the bottom platen was kept submerged in a water chamber located at the mould's base. The latter is a new feature introduced by Craciun et al. (2007). Prior to compaction, the material was mixed with the required amount of water and the moisture content (MC) was allowed to equilibrate for ~ 24 hours. Compaction was by falling hammer. A specimen was compacted in 7 layers using a pre-calculated amount of material for each layer. The top layer was calculated to reach ~20 mm above the required specimen height by the use of an extension collar. After compaction, the extension collar was removed, the surplus soil trimmed off, and the top surface levelled by rolling with a 25 mm diameter aluminium rod. Sandy UGB material passing 2.36 mm was used to level the top surface.

After levelling, the split mould was removed, top platen placed and the specimen sealed with a triaxial membrane. To avoid puncturing of the membrane during cyclic loading, a thin layer of liquid rubber was smeared on the internal surface of the triaxial membrane. This technique was developed and successfully verified by Lo et al. (1989).

### 3.4 Installation of Specimen

The procedure is schematically illustrated in Figure 1. Two 3 mm diameter rods were inserted into the side of the bottom platen to enable its transfer and placement onto the triaxial base without the need for touching the specimen. The bottom platen was connected to the drainage lines of the triaxial base by a "screw-in" connection. Note that the "screw-in" connector of the bottom platen has a conical porous tip to avoid trapping air bubbles while making the connection. While the bottom platen was turned onto the triaxial base, the bleeding valve was left slightly open to avoid any development of positive pore water pressure. After filling the cell chamber with water under a head of 1.5 m, a small vacuum of 5-10 kPa was applied via a vacuum regulator and the bottom drainage valve to burette was open. This induced a small amount of water flow out of the specimen. This movement of water was monitored by the burette reading.

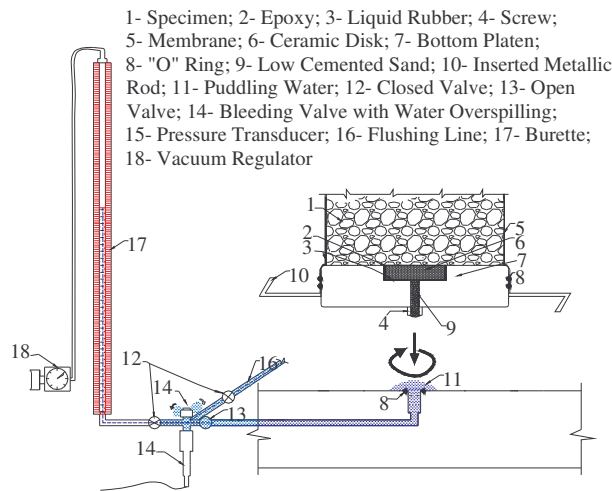


Figure 1. Installation of the specimen into triaxial base

### 3.5 Initialisation of Specimen

After overnight curing of the liquid rubber, the vacuum regulator was gradually increased to the required initial matric suction ( $S_i$ ). After about two days, when the flow of water had reduced to  $\sim 0.1$  ml / hour, the cell pressure was raised to 25 kPa. A further 1 to 2 days was needed to attain a "no flow" condition, under the same  $S_i$ . Initialisation was then complete. This initial condition was defined by 25 kPa isotropic net stress and prescribed  $S_i$ . This point is denoted as "I" on Figure 2.

The drainage valve to the burette was then closed and the specimen was therefore under constant MC. Then, the specimen was brought to an isotropic pressure of 70 kPa,

as denoted by point "O" on Figure 2. This condition was chosen as it approximately represented a more realistic stress path with changes in both radial and axial stress, denoted as **A'-B'** in Figure 2. This paper presents tests done only at simplified test condition denoted by path **A-B**.

To verify matric suction (S) equilibrium prior to cyclic loading, some specimens were monitored for 4-8 hours to detect any change in S. No more than 1 kPa fluctuation was measured, thus confirming the procedure and seal.

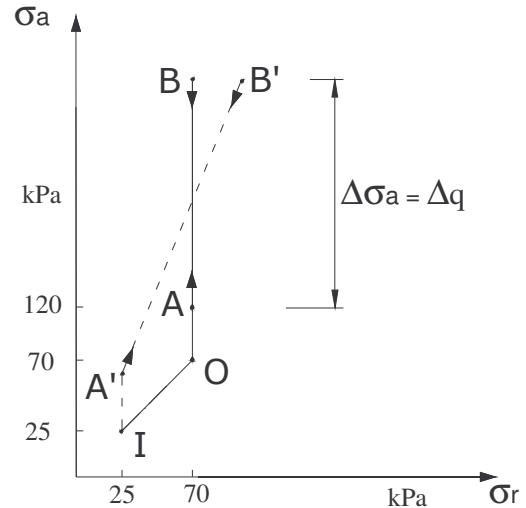


Figure 2. Stress path applied for UGB material testing

## 4 TESTING PROGRAM

### 4.1 Testing Conditions

The testing program is presented in Table 2. Note that the unit weight of **UGB-a** is higher than that of **UGB-b**.

The initial matric suction was selected based on a series of trials that established, approximately, the relationship between S and MC. Defining the initial state based on S allows more precise control of the initial condition.

### 4.2 Application of Cyclic Loading

After initialisation of the specimen at 25 kPa isotropic state, the cell pressure was increased at constant water content to 70 kPa. This is denoted as point "O" in Figure 2. A further waiting time of 8 hours was adopted to ensure S would equilibrate with the new cell pressure. Then the specimen was brought to an anisotropic state "A" ( $\sigma_a = 120$  kPa and  $\sigma_r = 70$  kPa), and cyclic loading commenced along the path **A-B**. The influence of different magnitudes of cyclic loading was examined by conducting tests with different  $\Delta q$ . Different values of  $\Delta q$  were achieved by changing the deviator stress value at "B".

The 1<sup>st</sup> 10 cycles of loading were conducted at a slower frequency of 0.01 Hz in order to allow the full development of virgin loading strain. This was then followed by  $2.8 \times 10^4$  haversine load cycles with a frequency of 0.3 Hz.

Table 2. Testing program

UGB-O density at MDD of this material = 2.313 g/cm <sup>3</sup>						
Test	$\Delta q$ (kPa)	$\sigma_r$ (kPa)	$S_i$ (kPa)	$MC_i$ (%)	C (%)	DOS (%)
CO1	360	70	55	3.57	100.3	39
CO2	450	70	55	3.64	99.7	38
CO3	540	70	- <sup>(1)</sup>	3.6	100.02	38
CO4	650	70	55	3.6	99.96	38
UGB-a density at MDD of this material = 2.51 g/cm <sup>3</sup>						
Test	$\Delta q$ (kPa)	$\sigma_r$ (kPa)	$S_i$ (kPa)	$MC_i$ (%)	C (%)	DOS (%)
CFa1	360	70	70	4.2	99.9	67
CFa2	450	70	70	4.17	100.3	69
CFa3	540	70	70	4.27	99.4	66
UGB-b density = 2.313 g/cm <sup>3</sup> = MDD of Original Material						
Test	$\Delta q$ (kPa)	$\sigma_r$ (kPa)	$S_i$ (kPa)	$MC_i$ (%)	C (%)	DOS (%)
CFb1	360	70	70	4.43	105	55
CFb2	540	70	70	4.5	100.02	45
CFb3	650	70	70	4.41	99.89	44

$\Delta q$  = magnitude of cyclic deviator stress  
 $\sigma_r$  = cell pressure  
 $S_i$  = initial matric suction  
 $MC_i$  = moisture content at initial condition  
 C = degree of compaction relative to tabulated MDD  
 DOS = degree of saturation  
<sup>1)</sup> = failure of matric suction measurement

5 ANALYSIS OF TEST RESULTS

The influence of additional fines was studied by analysing the test results in a comparative manner. Two sets of comparisons were made: i) **UGB-0** versus **UGB-a** and ii) **UGB-0** versus **UGB-b**. Each set of comparisons consisted of 3 pairs of tests conducted at different  $\Delta q$ . However, each pair of tests was conducted with identical cyclic loading. In presenting the test results, the following additional notations are used:

$\epsilon_a$  = Axial permanent strain (%)  
 $\epsilon_v$  = Volumetric permanent strain (%)  
 $M_R$  = Resilient modulus (MPa)  
 N = Number of loading cycles  
 Subscripts: "i" = initial  
 "o" = start of cyclic loading

5.1 Comparison 1: material **UGB-0** versus **UGB-a**

Both **UGB-0** and **UGB-a** were compacted to their respective MDD. **UGB-a** attained a higher dry density of 2.51g/cm<sup>3</sup>, even though the input compaction energy and compaction mode was identical. This is a direct result of the higher fines content. **UGB-a** also had a higher  $S_i$  as a result of the increase in fines content.

The  $\epsilon_a$  - N plots showing the development of axial strain with load cycles for the two materials are presented in Figure 3a. Note that N is plotted in log-scale.

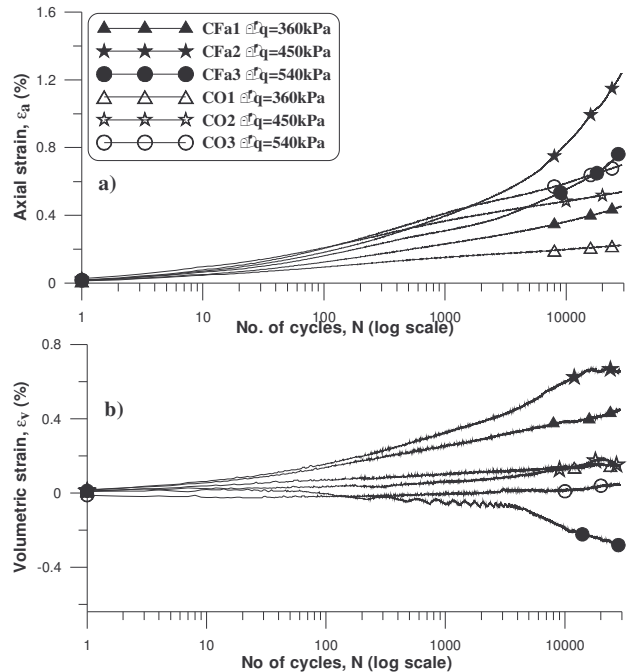


Figure 3. Axial and volumetric permanent strain responses of UGB-0 and UGB-a

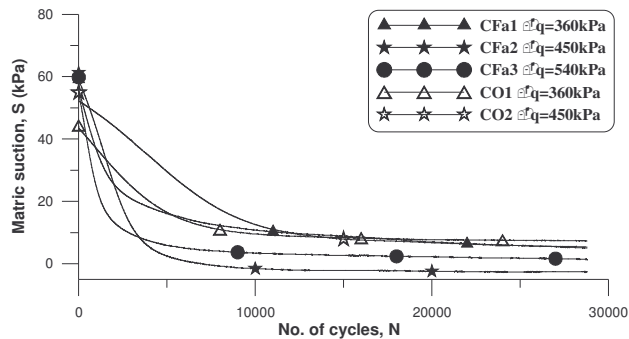


Figure 4. Matric suction responses for UGB-0 and UGB-a

**UGB-a** manifested a higher rate of accumulation of permanent axial strain when compared to that of **UGB-0** tested at the same  $\Delta q$ . Furthermore, the  $\epsilon_a$  - N curves of UGB manifested a convex upward shape whereas those of **UGB-a** manifested a concave upward shape. The latter is indicative of a less stable condition despite these specimens having had higher dry densities.

The  $\epsilon_v$  - N curves showing the development of volumetric strain with load cycles is presented in Figure 3b. For tests conducted at  $\Delta q$  of 360 kPa and 450 kPa, the permanent volumetric strain is always compressive for both specimen types. The rate of accumulation of volumetric strain for **UGB-a** is more pronounced than that of **UGB-0**. This is consistent with the relative trend for  $\epsilon_a$  - N curves. For the two tests conducted at the high  $\Delta q$  of 540 kPa, the accumulation of permanent volumetric strain

for **UGB-0** is negligible to slightly dilative. However, **UGB-a** manifested significant accumulation of dilative strain. This is indicative of a less stable behaviour despite **UGB-a** specimens having higher dry densities.

This apparently unexpected behaviour becomes evident when the matric suction response is examined in terms of  $S - N$  curves as presented in Figure 4. Note that  $N$  is plotted in linear scale as the change in matric suction with load cycles is more gradual relative to that of strain development. The  $S_o$  is less than  $S_i$  because the application of 70 kPa cell pressure (corresponding to "O") reduced slightly the matric suction. For **UGB-0** specimens the average value of  $S_o$  was about 50 kPa, while for **UGB-a** specimens was about 60 kPa. Therefore, the difference in matric suction between the two materials at the stage defined by "O" was less than that at state "I". For  $\Delta q$  of 450 kPa and 540 kPa, the reduction in matric suction for **UGB-a** was more significant than that of **UGB-0**. Thus eventually, the matric suction became less than that of **UGB-0**. For the test at  $\Delta q$  of 360 kPa, the matric suction of **UGB-a** eventually approached that of **UGB-0** for the complete test. (See Figure 4).

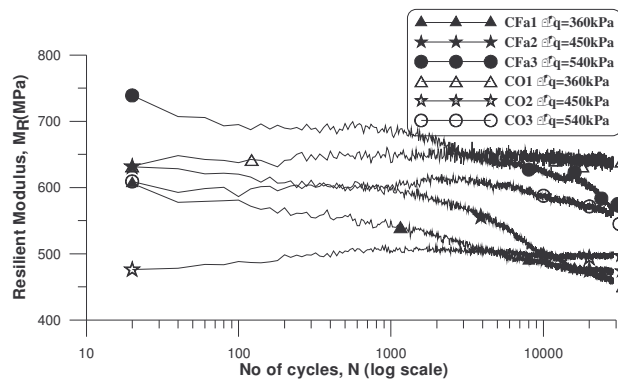


Figure 5. Resilient moduli responses for **UGB-0** and **UGB-a**

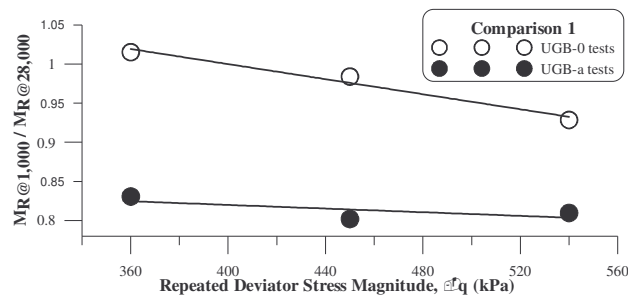


Figure 6. Degradation of  $M_R$  with  $\Delta q$  for Comparison 1

The  $M_R - N$  curves showing the evolution of resilient moduli with load cycles are presented in Figure 5. Note that in general,  $M_R$  may increase or decrease with  $N$  and therefore a simple statement of the relative resilient behaviour cannot be made. For  $N \leq 100$ , the resilient

moduli of **UGB-0** were either significantly smaller than, or approximately equal to, those of **UGB-a**. However, this statement cannot be generalised to higher  $N$  values. For the  $M_R - N$  curves of **UGB-0** at  $\Delta q$  of 360 kPa and 450 kPa, the resilient moduli showed little change with load cycle although some slight increase with  $N$  was manifested. For the test conducted at  $\Delta q$  of 540 kPa, the resilient modulus began to degrade gradually after 2000 load cycles. However, for **UGB-a**, the  $M_R - N$  curves for all 3 tests showed degradation from the very early stage of cyclic loading. In particular, the rate of degradation manifested by the **UGB-a** specimen at  $\Delta q = 360$  kPa was less than the other two tests after  $\sim 2000$  load cycles. At the end of the test ( $N = 28000$ ), the resilient moduli of **UGB-0** were higher than, or approximately equal to, those of **UGB-a**. This is a complete reversal in relative performance compared to that for  $N \leq 100$ . The rate of degradation of the two materials can be examined in closer detail by the ratio of  $M_R$  at  $N = 1000$  to that at  $N = 28000$ . The comparison is given in Figure 6. The **UGB-a** showed a more severe degradation.

The degradation of  $M_R$  with load cycles for **UGB-a** is in fact consistent with the matric suction response discussed earlier. At higher load cycles, the matric suction for **UGB-a** reduced more rapidly than that of **UGB-0**. This leads to a significant degradation in  $M_R$  values for **UGB-a**.

## 5.2 Comparison 2: **UGB-0** versus **UGB-b**

For this comparison, both materials were compacted to the same dry density (i.e. MDD found for **UGB-0**) at a MC of  $\sim 70\%$  from their respective OMC. **UGB-b** attained a higher  $S_i$  as a result of the increase in fines content.

The  $\epsilon_a - N$  plots showing the development of axial strain with load cycles for the two materials are presented in Figure 7a. For  $\Delta q = 540$  kPa the axial permanent strain of **UGB-b** material registered a slightly lower value when compared to **UGB-0**. However at  $\Delta q = 650$  kPa, a high rate of accumulation of axial strain,  $\epsilon_a$  is observed for both materials.

An exception to the above trend was for **UGB-b** at  $\Delta q = 360$  kPa. This specimen was compacted to 105 % to investigate any eventual effect. For this case the accumulated axial deformation at the end of test was more than double when compared to the corresponding test done on **UGB-0**. This means that the increase in dry density beyond a certain limit may have an unfavourable effect in material performance.

Volumetric strain is presented in Figure 7b. The  $\epsilon_v - N$  plots show a similar overall behaviour as depicted in  $\epsilon_a - N$  plots. For  $\Delta q$  values of 360 kPa and 540 kPa, **UGB-0** showed a small but gradual accumulation of compressive strain with  $N$  from the very beginning of the test. However for the same  $\Delta q$  values, **UGB-b** only started to accumulate measurable compressive volumetric strain after  $10^4$  cycles. At  $\Delta q = 650$  kPa, both materials showed volumetric dilative strain from the first onset. For **UGB-b**, the rate of dilative strain was more pronounced indicating a less stable condition.

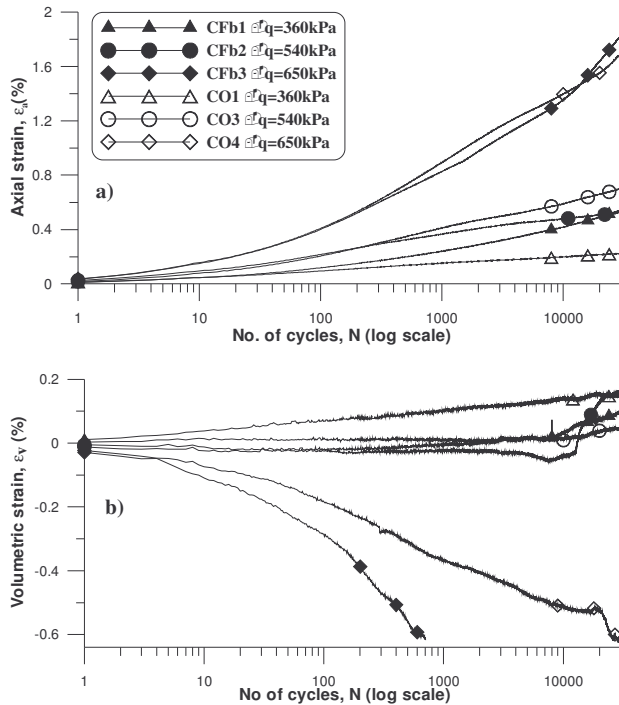


Figure 7. Axial and volumetric permanent strain responses of **UGB-0** and **UGB-b**

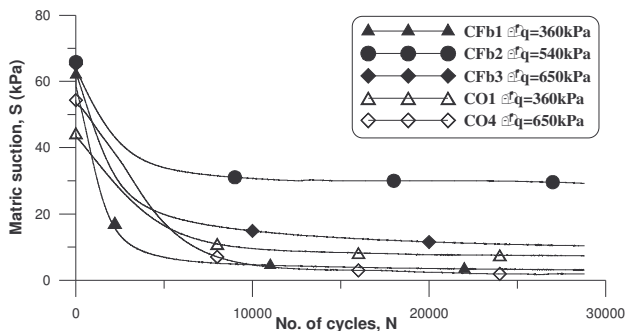


Figure 8. Matric suction responses for **UGB-0** and **UGB-b**

Matric suction behaviour with cyclic loading is presented in Figure 8. For this comparison, the difference in matric suction between the two materials was about the same at both stages “I” and “O”. This was due to a higher  $S_0$  value for **UGB-b** specimens, with an average of 66 kPa, [except for the test which achieved 105 % (i.e. CFb1) which will be discussed below]. The  $S - N$  curves show larger values of matric suction for **UGB-b** when compared with **UGB-0**. This behaviour is consistent with the good axial strain accumulation performance of **UGB-b** relative to the **UGB-0**.

Again, the exception was the test done at  $\Delta q = 360$  kPa on **UGB-b** material. Interesting to notice is that the 105 % compaction of this specimen increased the DOS with about 10 % (see Table 2) and registered an  $S_0$  value of 62 kPa. Therefore,  $S$  dropped significantly from the very beginning of cyclic loading, even if  $\Delta q$  for this test had the

lowest value. This particular case is consistent with the behaviour of **UGB-a** from Comparison 1 where the increase in dry density can accentuate the reduction in  $S$  with load cycles.

The  $M_R - N$  curves showing the evolution of resilient moduli with load cycles are presented in Figure 9. Higher values of moduli were obtained by **UGB-b** material when compared to **UGB-0** for the  $\Delta q$  values of 540 kPa and 650 kPa. However, for these  $\Delta q$  values, both materials manifested a similar gradual degradation with  $N$  after 2000 cycles.

The exception was for  $\Delta q = 360$  kPa for **UGB-b** which showed large degradation in  $M_R$  after only 300 cycles. Note that for the same  $\Delta q$  value **UGB-0** had the highest  $M_R$  value from all tests and showed no signs of degradation.

The degradation of moduli with  $N$ , presented in Figure 10, can be examined in detail with the ratio of  $M_R$  at  $N = 1000$  to that at  $N = 28000$  (end of test). It can be seen that both materials registered a similar rate of degradation relative to  $\Delta q$  magnitude. The poor performance of test reference (**UGB-b** test compacted to 105 %) is obvious and has about the same degradation as for **UGB-a**. Interestingly, the inferior resilient modulus characteristics of this test are only indicated clearly by the significant reduction of matric suction with  $N$ .

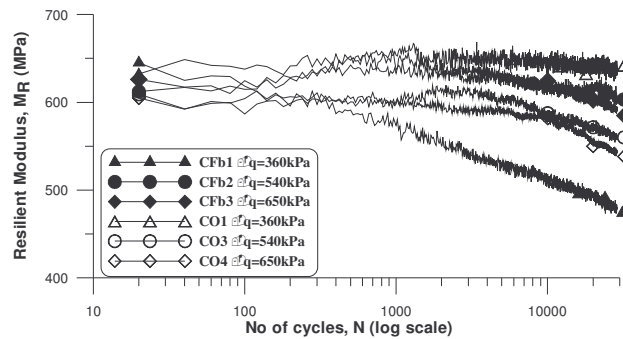


Figure 9. Resilient moduli responses of **UGB-0** and **UGB-b**

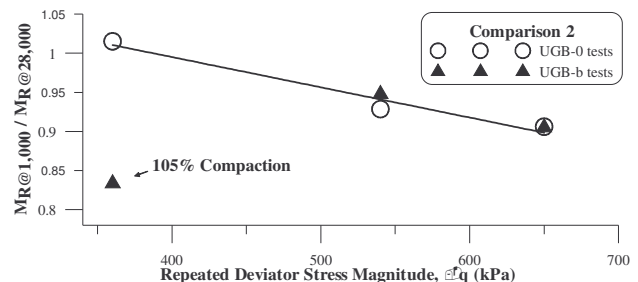


Figure 10. Degradation of  $M_R$  with  $\Delta q$  for Comparison 2

## 6 CONCLUSIONS

A set of conclusions regarding the influence of fines on an UGB material behaviour under cyclic loading are as follows

- It is important to have cyclic loading test results over a large number of load cycles. This is important because some statements about the relative performance of different materials are dependent on the number of load cycles. Furthermore, a change in the trend of relative performance may occur only after a large number of load cycles.
- The matric suction response can explain some unexpected behaviour. In particular, the significant drop in matric suction is linked with resilient modulus degradation, especially for the case when axial and volumetric strains do not provide clear information. This implies that matric suction response can be used effectively to rank material behaviour.
- A higher dry density does not necessarily correspond to a better behaviour (in terms of permanent strain accumulation and resilient modulus) under cyclic loading. For a material with higher density, degree of saturation increases more rapidly with volumetric compression that develops with load cycles. This rapid increase of degree of saturation will lead to a rapid drop in matric suction which in turn affects behaviour.

## REFERENCES

- Ashtiani, R. S., Little, D. N. and Masad, E. 2007. Evaluation of the impact of fines on the performance of lightly cemented stabilized aggregate systems, TRB 86th Annual Meeting, Transportation Research Board, Washington, DC, USA, TRB 2007 Annual Meeting CD-ROM: 26 pages.
- Chen, D. H., Chen, T. T., Scullion, T. and Bilyeu, J. 2006. Integration of field and laboratory testing to determine the causes of a premature pavement failure, Canadian Journal of Civil Engineering, 33: 1345-1358.
- Craciun, O., Lo, S. R. and Gnanendran, R. 2007. Deformation and matric suction response of unbound granular base materials subject to repetitive loading, 16th Southeast Asian Geotechnical Conference, Kuala Lumpur, Malaysia, 381-386.
- Fredlund, D. G. and Rahardjo, H. 1993. Soil mechanics for unsaturated soils, John Wiley and Sons, Inc. New York, NY, USA.
- Fwa, T. F. 1987. Water-induced distress in flexible pavement in a wet tropical climate, Transportation Research Record, 57-65.
- Haynes, J. H. and Yoder, E. J. 1963. Effects of repeated loading on gravel and crushed stone base course materials used in the AASHO road test, Transportation Research Record, 82-96.
- Hicks, L. D. 1956. Design and construction of base courses, 35th Annual Meeting, Highway Research Board Bulletin, Washington, DC, USA, 1-9.
- Hicks, R. G. and Monismith, C. L. 1971. Factors influencing the resilient properties of granular materials, Hwy. Res. Rec., 15-31.
- Kalcheff, I. V. 1974. Characteristics of graded aggregates as related to their behaviour under varying loads and environments, Utilization of Graded Aggregate Base Materials in Flexible Pavements, Oak Brook, Illinois, 8: 1-32.
- Lo, S.-C. R., Chen, K. 1999. Strain responses of granular base materials in stress path cyclic triaxial testing, J. of Transportation Research Record, 66-74
- Lo, S.-C. R., J., C. and Lee, I. K. 1989. A technique for reducing membrane penetration and bedding errors, Geotechnical Testing Journal, 12: 311-316.
- Thom, N. H. and Brown, S. F. 1988. The effect of grading and density on the mechanical properties of a crushed dolomitic limestone, 14th ARRB Conference, 14, part 7: 94-100.
- Thompson, M. R. and Smith, K. L. 1990. Repeated triaxial characterization of granular bases, Transportation Research Record, 7-17.
- Yoder, E. J. and Woods, K. B. 1946. Compaction and strength characteristics of soil aggregates mixtures, Proceeding of the Annual Meeting, National Academy of Sciences - National Research Council, Washington, DC, USA., 26: 511-520.